GeoHealth

RESEARCH ARTICLE
10.1029/2022GH000601

Key Points:

- Achieving climate change mitigation and sustainable development goals greatly reduces premature deaths due to air pollution in Africa
- Cumulative avoided premature deaths surpass one million for Northern, West, and East Africa in the 2030s, and for all regions by 2050
- Projected changes in exposure vary by up to 50% across models for a given scenario and region, but health impacts only vary by up to 35%

Correspondence to:
D. Shindell,
drew.shindell@duke.edu

Citation:
Shindell, D., Faluvegi, G., Parsons, L., Nagamoto, E., & Chang, J. (2022). Premature deaths in Africa due to particulate matter under high and low warming scenarios. *GeoHealth*, *6*, e2022GH000601. https://doi.org/10.1029/2022GH000601

Received 2 FEB 2022
Accepted 19 APR 2022

Author Contributions:
Conceptualization: D. Shindell
Formal analysis: G. Faluvegi, E. Nagamoto, J. Chang
Funding acquisition: D. Shindell
Investigation: D. Shindell, G. Faluvegi, L. Parsons, E. Nagamoto, J. Chang
Methodology: D. Shindell, G. Faluvegi, L. Parsons
Project Administration: D. Shindell
Supervision: D. Shindell, L. Parsons
Validation: D. Shindell, G. Faluvegi
Visualization: D. Shindell, G. Faluvegi, L. Parsons, E. Nagamoto, J. Chang
Writing – original draft: D. Shindell
Writing – review & editing: G. Faluvegi, L. Parsons, E. Nagamoto

Premature Deaths in Africa Due To Particulate Matter Under High and Low Warming Scenarios

D. Shindell[1], G. Faluvegi[2,3], L. Parsons[1], E. Nagamoto[1], and J. Chang[1]

[1]Nicholas School of the Environment, Duke University, Durham, NC, USA, [2]Center for Climate Systems Research, Columbia University, New York, NY, USA, [3]NASA Goddard Institute for Space Studies, New York, NY, USA

Abstract Sustainable development and climate change mitigation can provide enormous public health benefits via improved air quality, especially in polluted areas. We use the latest state-of-the-art composition-climate model simulations to contrast human exposure to fine particulate matter in Africa under a "baseline" scenario with high material consumption, population growth, and warming to that projected under a sustainability scenario with lower consumption, population growth, and warming. Evaluating the mortality impacts of these exposures, we find that under the low warming scenario annual premature deaths due to $PM_{2.5}$ are reduced by roughly 515,000 by 2050 relative to the high warming scenario (100,000, 175,000, 55,000, 140,000, and 45,000 in Northern, West, Central, East, and Southern Africa, respectively). This reduction rises to ~800,000 by the 2090s, though by that time much of the difference is attributable to the projected differences in population. By contrast, during the first half of the century benefits are driven predominantly by emissions changes. Depending on the region, we find large intermodel spreads of ~25%–50% in projected future exposures owing to different physics across the ensemble of 6 global models. The spread of projected deaths attributable to exposure to fine particulate matter, including uncertainty in the exposure-response function, are reduced in every region to ~20%–35% by the non-linear exposure-response function. Differences between the scenarios have an even narrower spread of ~5%–25% and are highly statistically significant in all regions for all models. These results provide valuable information for policy-makers to consider when working toward climate change mitigation and sustainable development goals.

Plain Language Summary The economies in many low- and middle-income countries in Africa are heavily reliant on fossil fuel consumption; many of these countries are on development trajectories that will lead to increased fossil fuel use in the future. Burning fossil fuels produces air pollution, such as fine particulate matter, that has large-scale health consequences. However, reduced fossil fuel consumption under more sustainable and climate-friendly development pathways has the potential to provide enormous public health benefits via reduced air pollution, especially in currently polluted regions. We examine changes in human exposure to air pollution, and associated premature deaths, in various regions in Africa under a future scenario with high consumption, population growth, and warming, and under a more sustainable scenario with lower consumption, population growth, and warming. We find that under the low warming scenario, premature deaths due to air pollution are reduced by about half a million people per year by 2050 relative to the high warming scenario. Benefits are especially large in West and East Africa, dominated by Nigeria and by Ethiopia and Uganda/Rwanda/Burundi, respectively. These findings provide information for policy-makers to consider when working toward climate change mitigation and sustainable development goals.

1. Introduction

Globally, air pollution leads to a vastly larger public health burden than climate change does at present. The annual toll of premature deaths due to air pollution is estimated to be around 8–10 million (Burnett et al., 2018; Vohra et al., 2021) whereas the current toll from climate change is estimated in the hundreds of thousands (Romanello et al., 2021; World Health Organization, 2014). As many sources of the emissions that drive climate change, such as fossil fuel burning, are the same sources that cause air pollution, efforts to reduce climate change will also often benefit air quality. While climate change and sustainable development have been high on the international policy agenda and widely studied in the scientific community, there has been less effort to use the vast quantities of climate-related data to evaluate the so-called "co-benefits" for air quality of actions to mitigate climate change and achieve sustainable development.

Along with many other low- and middle-income countries, many parts of Africa suffer from both some of the world's worst air quality (Burnett et al., 2018; Petkova et al., 2013) and from some of the most pronounced damages due to climate change (Ranasinghe et al., 2021). In addition, due to the relatively low income levels in much of Africa, populations tend to be more vulnerable to both the health impacts of air pollution and climate disruptions (Ranasinghe et al., 2021; Stanaway et al., 2018). African policymakers must face both these environmental challenges while also working toward the development goals leaders have set to improve economic and social conditions for their citizens, such as the African Union's Agenda 2063 (African Union Commission, 2015). Fortunately, the drive toward sustainable development and climate change mitigation is likely to greatly improve Africa's air quality, leading to large public health benefits. In addition to the phasing out of fossil fuels required to meet climate goals, achievement of sustainable development goals, especially the provision of access to clean energy, would reduce use of biofuels, leading to substantial additional air quality improvements in Sub-Saharan Africa. Hence this region is one that is likely to experience some of the greatest air quality-related benefits from policies to promote sustainable development and climate change mitigation.

We therefore take advantage of the availability of a large number of simulations of future atmospheric composition under two 21st century development and emissions pathways to examine the potential impact of climate change mitigation on premature mortalities due to exposure to fine particulate matter in Africa. The simulations were those performed to support the Intergovernmental Panel on Climate Change under the Coupled Model Intercomparison Project's Phase 6 (CMIP6). These were driven by emissions trajectories created under the Shared Socio-economic Pathway (SSP) framework (Riahi et al., 2017). Within those, we analyze the effects of a worldwide transition to a sustainable development trajectory called SSP1 under a low warming (roughly 2°C in 2100) scenario labeled 2.6 for the radiative forcing reached in 2100 (hereafter SSP1_2.6). This scenario envisions a world focused on achievement of sustainable development goals, with moderate population growth and gradual reductions in energy and resource intensity. For comparison, we also analyze another scenario, SSP3, under which development trajectories around the world are highly fragmented with many areas not transitioning to sustainable development. In the SSP3 scenario, emissions remain high and radiative forcing reaches 7.0 W/m^2 in 2100 (leading to warming of around 3–4°C; hereafter SSP3_7.0). Under this scenario, investments in education decline and population growth in developing countries is therefore large.

The difference between these scenarios provides a view of how climate change mitigation, as well as a more general transition to sustainable development, affect air pollution. We compare air pollution across the six CMIP6 models that provided surface aerosol fields which allowed for the construction of fine particulate matter fields for both SSP1_2.6 and SSP3_7.0 (Turnock et al., 2020). The use of multiple CMIP6 models allows us to characterize the uncertainty associated with our understanding of the physical response of the Earth system to the differing emissions. The six models used here roughly span the range of fine particulate matter seen in the 11 models with available historical simulations, suggesting they are likely to provide a reasonable characterization of the larger ensemble. The scenarios diverge in 2016, so that there are already differences by the present year, but we use those to leverage the multi-model simulations available from CMIP6 since simulations with newer scenarios that would be identical through the present-day are not yet available. However, this implies that our future projections include a modest amount of emissions changes that are already presumed to have taken place over the past ∼5 years.

Our analysis focuses on the impacts of particulate matter with a diameter of 2.5 microns or less ($PM_{2.5}$) on premature death. Exposure to $PM_{2.5}$ has many additional morbidity health impacts, and there are mortality effects from both ozone exposure and climate change itself, so this study is not meant to be exhaustive. The mortality burden from $PM_{2.5}$ tends to be far larger than those from other environmental factors (Romanello et al., 2021), however, and so provides insight into the largest health-related benefit likely to occur from climate change mitigation, at least in the near-term. We find that projected reductions in $PM_{2.5}$ exposure under low warming scenarios could prevent millions of premature deaths across Africa, indicating that even though we analyze only this one impact the results may be a valuable contribution to policy-makers and the public.

2. Modeled $PM_{2.5}$ and Evaluation Against Near-Present Day Observations

$PM_{2.5}$ has been analyzed previously in CMIP6 models (Turnock et al., 2020), and we utilize those "raw" fields in our estimates. In that analysis, $PM_{2.5}$ was defined as the sum of aerosol masses:

$$PM_{2.5} = BC + OA + SO4 + (0.25 \times Sea - Salt) + (0.1 \times Dust) \quad (1)$$

where BC is Black Carbon, OA are Organic Aerosols, and SO4 is Sulphate. We perform a two-part process to debias and downscale these "raw" fields, creating what we refer to as "unbiased" fields. First, we note that in the raw fields, nitrate was excluded as few models provided nitrate simulations, and the assumption of a uniform fraction of sea-salt and mineral dust being less than or equal to the 2.5 micron cutoff was required as size-resolved information was also not provided in CMIP6. The first part of our process is debiasing, in which we adjust these CMIP6 $PM_{2.5}$ fields using output from the GISS model (Kelley et al., 2020), which simulates both nitrate and size-resolved dust (and uses a smaller fixed portion of small sea-salt, 0.1, as $PM_{2.5}$). Specifically, we calculated the ratio of the GISS $PM_{2.5}$ including the model's nitrate and size-resolved local dust fraction ≤2.5 microns to its $PM_{2.5}$ using the definition given in Equation 1. Secondly, within the GISS model we have developed a method to simulate $PM_{2.5}$ at higher resolution, utilizing higher-resolution emissions data and the first-order horizontal moments of the native grid box resolution tracers. This has been shown to improve the realism of the model's $PM_{2.5}$, especially in urban areas (Shindell et al., 2018). The second part of our adjustment process is downscaling, for which we reran the 2015–2019 period with the same GISS-E2-1-G model used for CMIP6 but this time including the high-resolution $PM_{2.5}$ method and calculated the ratio of simulated $PM_{2.5}$ in each 0.5 × 0.5° grid box to that in the native 2 × 2.5° box. We then multiplied all models' $PM_{2.5}$ by that ratio and the debiasing ratio during the transformation to a common 0.5 × 0.5 grid. These adjustments naturally are dependent upon the realism of the GISS model used to create the gridded scalings applied to all other models, but we have evaluated the high-resolution GISS $PM_{2.5}$, including the model's nitrate and internally-defined fine-mode dust loading, and found it generally agrees well with observations (Shindell et al., 2018).

We compare CMIP6 $PM_{2.5}$ data with observations as near to 2015 as practical to evaluate the ability of CMIP6 models to simulate observed local $PM_{2.5}$ before and after unbiasing. We use measurements from ground monitors for the early 2010s (largely 2013–2015) as assembled by the World Health Organization (WHO, 2016), including in our global analysis only those stations that directly measured $PM_{2.5}$ rather than those estimating $PM_{2.5}$ from PM_{10} measurements. We also compare with estimates for 2014–2016 derived from a chemistry-transport model for which simulated $PM_{2.5}$ has been adjusted to match satellite AOD measurements (e.g., adjusted $PM_{2.5}$ = modeled $PM_{2.5}$ × satellite AOD/modeled AOD) (Shaddick et al., 2018; hereafter referred to as "model + satellite AOD" where the model in that case is not a CMIP6 model). This data set provides nearly complete global coverage, but the estimates depend upon the underlying model correctly capturing the relationship between surface $PM_{2.5}$ and column AOD that is used in the adjustment process as well as the satellite accurately measuring AOD, which can be especially challenging in regions with persistent clouds or complex surface albedo. In our analysis, inland values are based on bilinear interpolation of the original 0.1 × 0.1° data whereas coastal values are averages over 0.1 × 0.1° cells with non-zero values since oceanic areas are reported as zero. In practice, though model + satellite AOD data are far more extensive in their geographic coverage, they often show substantial biases relative to ground-based monitors (e.g., Alvarado et al., 2019).

As we are focused on health impacts in this study, we evaluate biases in population-weighted $PM_{2.5}$ to reflect human exposure. We use population data for 2015 from the Gridded Population of the World (GPWv3; updated from CIESIN, 2005). In Table 1 we show that globally, the raw modeled $PM_{2.5}$ is biased low by a large amount in comparison with observations, on average more than 50% relative to either WHO ground monitors or model + satellite AOD. This is expected due to the absence of some components and is consistent with prior evaluations (e.g., Turnock et al., 2020). After our unbiasing process the average bias of global population-weighted $PM_{2.5}$ across the models is +26% relative to ground monitors and −14% relative to the model + satellite AOD data set. This suggests that there is no clear indication of any residual bias versus observations after our unbiasing procedure, and that the unbiasing procedure, on average, reduces CMIP6 $PM_{2.5}$ bias relative to the raw CMIP6 $PM_{2.5}$. We note that results from the two SSPs are extremely similar for this 2015–2019 period, with average differences in population-weighted values over Africa across the 6 models of 1.2 and 0.8 μg m^{-3} at the locations of ground monitors and model + satellite AOD datasets, respectively, with SSP1 nearly always slightly smaller than SSP3.

Globally, population-weighted $PM_{2.5}$ concentrations in the CMIP6 models fall broadly into two categories: a lower concentration group (GISS, MIROC and NorESM2) and a higher concentration group (GFDL, MRI and UKESM1). Sampling the CMIP6 models at the sites of WHO surface monitors (N = 1297, where N is the number

Table 1
Modeled and Observed Population-Weighted $PM_{2.5}$ ($\mu g\ m^{-3}$) at Measurement Sites; Global

CMIP6 model	Observed PM	Unbiased CMIP6 modeled PM	Bias versus observed	Raw CMIP6 modeled PM	Bias versus observed
	WHO ground				
GFDL-ESM4	**38.9**	**54.1**	**15.1**	**18.1**	**−20.8**
GISS-E2-1-G	**38.9**	**38.3**	**−0.6**	**13.2**	**−25.8**
MIROC-ES2L	**38.9**	**37.6**	**−1.4**	**12.6**	**−26.3**
MRI-ESM2-0	**38.9**	**62.0**	**23.0**	**21.1**	**−17.9**
NorESM2-LM	**38.9**	**39.7**	**0.8**	**13.9**	**−25.0**
UKESM1-0-ll	**38.9**	**63.4**	**24.4**	**21.0**	**−18.0**
Average	**38.9**	**49.2**	**10.2**	**16.6**	**−22.3**
	Model + satellite AOD				
GFDL-ESM4	**50.4**	**46.3**	**−4.1**	**18.6**	**−31.8**
GISS-E2-1-G	**50.4**	**32.3**	**−18.1**	**13.2**	**−37.2**
MIROC-ES2L	**50.4**	**31.1**	**−29.3**	**12.8**	**−37.9**
MRI-ESM2-0	**50.4**	**53.5**	**3.1**	**21.6**	**−28.8**
NorESM2-LM	**50.4**	**38.9**	**−11.5**	**16.3**	**−34.0**
UKESM1-0-ll	**50.4**	**58.5**	**8.1**	**23.5**	**−26.9**
Average	**50.4**	**43.4**	**−7.0**	**17.6**	**−32.8**

Note. Modeled values are averages over 2015–2019 from both SSP1_2.6 and SSP3_7.0 simulations. Ground-based data is primarily from 2013 to 2015 and model + satellite AOD estimates are averages over 2014–2016. Models are in alphabetical order with models having smaller values (<45 $\mu g\ m^{-3}$ at the WHO ground sites) underlined.

of grid boxes with at least one observation), the models with lower concentrations show good agreement at the global level, whereas the group with higher concentrations overpredicts $PM_{2.5}$ by about 50% (Figure 1). However, when sampling the CMIP6 models at sites with PM data from the model + satellite AOD data set (N = 60,859) the situation is exactly the opposite; the higher concentration group matches the model + satellite-based concentrations well, whereas the low concentration group underpredicts by ∼33%. We note that comparing the two datasets at the 1297 locations with both ground and model + satellite AOD data there is no clear bias (<1 $\mu g\ m^{-3}$). This suggests that the models in the group with lower concentrations tend to do a better job in areas of the world with many monitors (Europe, North America, China, Korea and Japan) whereas the higher concentration group may perform better in regions with few monitors (Africa, South and Southeast Asia, former Soviet Union, and most of Latin America), though the reliability of the data is lower in the latter regions and the model + satellite AOD data set may overpredict $PM_{2.5}$.

Turning to Africa, ground-based monitoring data are quite sparse (Petkova et al., 2013), and the WHO data set includes only 29 sites for the entire continent that directly measure $PM_{2.5}$. We therefore include both direct $PM_{2.5}$ measurements and values converted from PM_{10} observations for this analysis, which expands the data availability to 42 sites (Mauritius is excluded as a sparsely populated remote island). This allows us in particular to include substantially more information from North Africa, which has only a single site that directly measures $PM_{2.5}$. We also include 13 monitors located on US Embassies in Africa (available at: https://www.airnow.gov/international/us-embassies-and-consulates/), of which two are located within the same grid box as data points in the WHO data set (i.e., bringing in 11 new locations and changing the average for two existing locations). Including converted PM_{10} measurements from the WHO, the data set includes observations in Egypt, Tunisia and Morocco, while the US Embassy data set includes Algeria and Sudan, so that coverage is much more widespread across North Africa (Figure 2).

The pattern in the CMIP6 model/observation comparison for African locations only is similar to that seen at the global level. The group of CMIP6 models with lower concentrations is in fairly good agreement with the surface monitors, and the higher concentration group generally overpredicts concentrations (Figure 3). The one exception

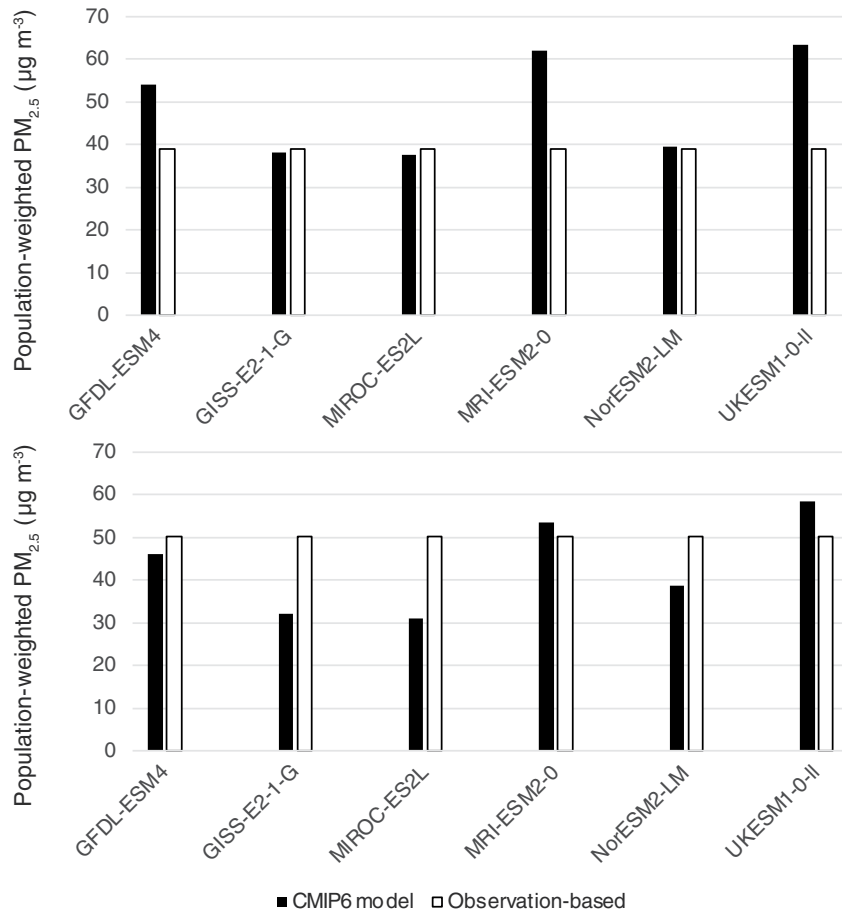

Figure 1. Worldwide population-weighted $PM_{2.5}$ from ground monitors (top; N = 1,297) and model + satellite AOD estimates (bottom; N = 60,859) compared with the values in the indicated Coupled Model Intercomparison Project's Phase 6 (CMIP6) models after unbiasing and sampling at the same locations.

is the NorESM2 model, which was in the low group at the global level but falls somewhere between the groups in the Africa analysis. The GISS and MIROC models, which remain clearly in the lower group, show values very similar to the surface observations. The models with higher $PM_{2.5}$ levels at these 53 sites, especially UKESM1, appear to greatly over predict in comparison with ground-based observations. However, when comparing with the model + satellite AOD estimates over Africa, it is the models with the highest exposures that appear to best match the observations and even the highest exposures in the unbiased models are still less than the model + satellite-based estimates (Figure 3, bottom).

Unlike the global case that showed no consistent bias between the model + satellite AOD data set and the ground monitors, when we compare them at these 53 African sites, the model + satellite AOD data set is substantially high biased: 21 µg m^{-3} for the population-weighted mean. Restricting the comparison to the 40 sites with direct $PM_{2.5}$ observations the bias is still large at 16 µg m^{-3}. These biases are ~45% of the population-weighted means from either set of ground monitors. This suggests that the model + satellite AOD data may be broadly biased high across Africa, consistent with prior analyses reporting biases in estimates based on satellite AOD for urban areas in Africa of −31 to +23 µg m^{-3} due to significant challenges using such methods in coastal and dusty areas (Alvarado et al., 2019).

Thus the evaluation over Africa indicates that the unbiased models largely fall between the lower exposure estimates based on surface monitors and the potentially high-biased estimates based on model + satellite AOD. This suggests that the unbiased models do a reasonable job of capturing the range of probable current population-weighted $PM_{2.5}$ exposures based on limited observations, but that the results of the "low" group of models

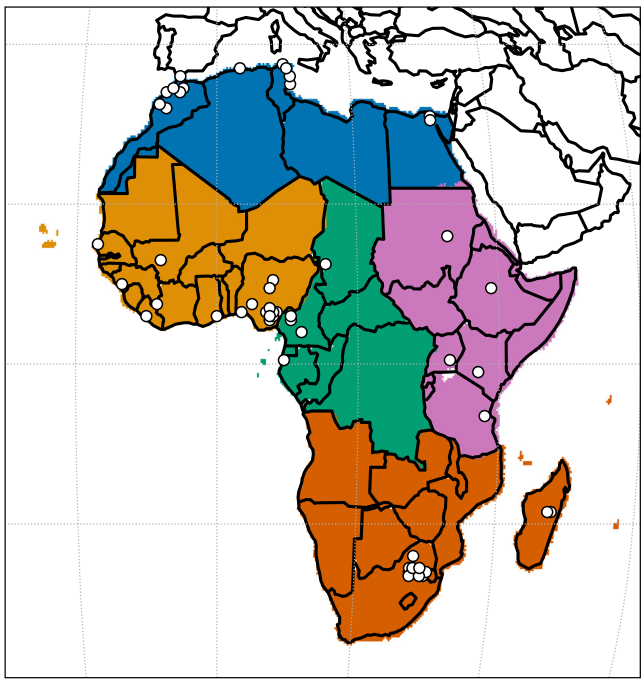

Figure 2. The locations of the ground monitors over Africa used in the model evaluation (white dots) along with the five African regions used in this study (Northern in blue, West in gold, Central in green, East in purple, Southern in orange/red).

may be more reliable over Africa given the bias in the model + satellite AOD data set. We note that the locations with surface observations are quite skewed toward locations with high $PM_{2.5}$ levels in the models, with population-weighted values at those 53 locations ~30%–80% higher than population-weighted modeled values over the entire continent (Figure 3). In contact, those locations show the same average population-weighted values of 64 μg m^{-3} in the model + satellite AOD data set as the whole continent. If the models are correct in reporting higher values in the urban centers where most monitors are located that would again suggest there are problems with the model + satellite AOD data set. Additional monitors located further away from urban areas would be valuable to provide a better understanding of exposure averages over the continent, though understandably authorities may be most interested in monitoring in comparatively polluted areas.

In addition to comparing their near-present climatologies against observations, models are often evaluated by examining their historical trends. Unfortunately, historical trends in surface $PM_{2.5}$ are not available for virtually any locations in Africa. Examination of trends in fine mode AOD, were future models to save that quantity, against AeroNet observations could provide additional useful constraints, however (Mortier et al., 2020).

3. Emissions Projections Under Low and High Warming Scenarios

Differences between emissions projected under the low warming scenario (SSP1_2.6) and those under the high warming scenario (SSP3_7.0) will be a major driver of differences in $PM_{2.5}$ exposure (along with population and vulnerability changes). We therefore present a brief overview of emissions trends for several of the main $PM_{2.5}$ precursors. Changes in aircraft and natural emissions, including Biogenics and lightning, are not included in this analysis, but we do include emissions from biomass burning. For visual clarity, we divide Africa into five contiguous regions (Figure 2), and then examine the temporal evolution of emissions in those regions (Figure 4). The trends in aerosol precursors vary by emitted species, region, and scenario in complex ways. Black carbon emissions are similar to those for organic carbon and have a smaller magnitude, and so are not shown.

Beginning with the high warming scenario (SSP3_7.0), sulfur dioxide emissions decrease over the long term in Southern Africa following a mid-century peak, stay roughly level in Central Africa, and increase in the other three regions. Black carbon emissions similarly show trends in different directions across regions. By contrast, ammonia emissions rise in all areas under SSP3_7.0. In the low warming scenario (SSP1_2.6), SO_2 emissions decrease in most regions, except Southern Africa, which does not show large-scale decreases until the end of the century. Organic carbon emissions decrease rapidly under this scenario in all regions by 2030, but thereafter exhibit varying trends (though changes are typically small). Ammonia emissions increase under the low warming scenario.

Comparison of the two scenarios shows that emissions of all aerosol precursors are nearly always lower under SSP1_2.6 than SSP3_7.0. However, the temporal evolution of those differences varies greatly across species. In particular, there are rapid drops then a leveling off of differences in carbonaceous aerosol precursors. By contrast, there are steady declines in the differences for ammonia, and declines in the differences occur quite late in the century for sulfur dioxide, except for North Africa. In the two cases in which emissions are higher under SSP1_2.6 than SSP3_7.0 (e.g., organic carbon in Southern Africa and ammonia in North Africa), higher emissions could be due to the different models used in generating these scenarios (AIM for SSP3 and IMAGE for SSP1). The IMAGE model shows complex trends in Southern Africa in particular that are difficult to account for, including the mid-century increase in SO_2 emissions that is almost entirely driven by a very small area at the Zambia/Congo border (Figure 5, right) and comes from the industrial sector. Aside from that anomaly, the

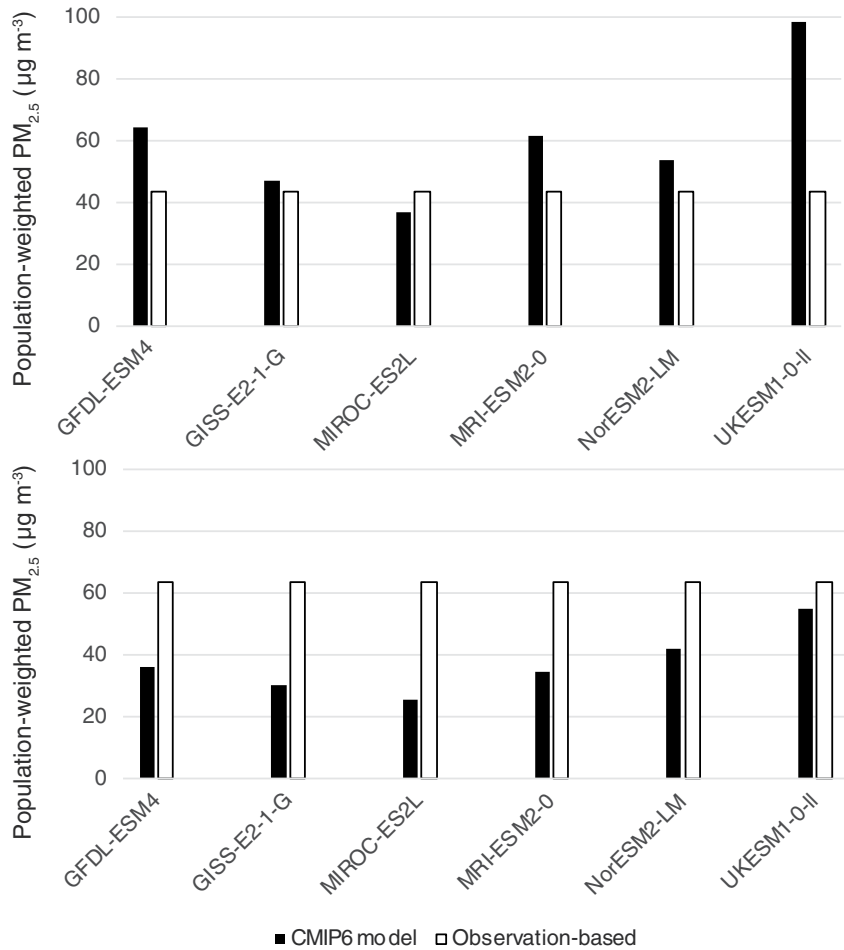

Figure 3. Population-weighted $PM_{2.5}$ from ground monitors in Africa (top; N = 53) and model + satellite AOD estimates (bottom; N = 10,641) over Africa compared with the values in the indicated Coupled Model Intercomparison Project's Phase 6 (CMIP6) models after unbiasing and sampling at the same locations.

increases in both organic carbon in Southern Africa and ammonia in North Africa under SSP1_2.6 relative to SSP3_7.0 are, however, very small and contribute little to total changes in $PM_{2.5}$.

Although it is impractical to look at temporal trends for every country within Africa, it is important to note that the regional trends are in several cases dominated by changes in one or a few countries. For example, the spatial pattern of black carbon emissions differences in 2050 (Figure 5, left) shows that West Africa is dominated by changes in Nigeria, and North Africa is dominated by changes in Egypt, whereas East Africa includes large and discrete changes in both Ethiopia and areas near Lake Victoria (Uganda, Rwanda, Burundi and parts of Tanzania). These correspond to locations with the highest levels of BC emissions both at present and in 2050 under SSP3_7.0. In contrast, no single countries in Central or Southern Africa stand out as having such large changes in BC emissions.

The benefits of improved air quality will follow these national-level changes, and will be driven by different sectors. Benefits in Nigeria, Ethiopia, Uganda, Rwanda, Burundi and Tanzania will stem largely from the residential sector, which dominates total reductions in emissions of BC and OC and also makes substantial contributions to VOC reductions. Benefits in countries including South Africa will be largely driven by reductions in energy sector emissions of SO_2 and NO_x, and Egypt will be affected by both these sectors. In contrast, reductions in transport and agricultural emissions play a lesser role.

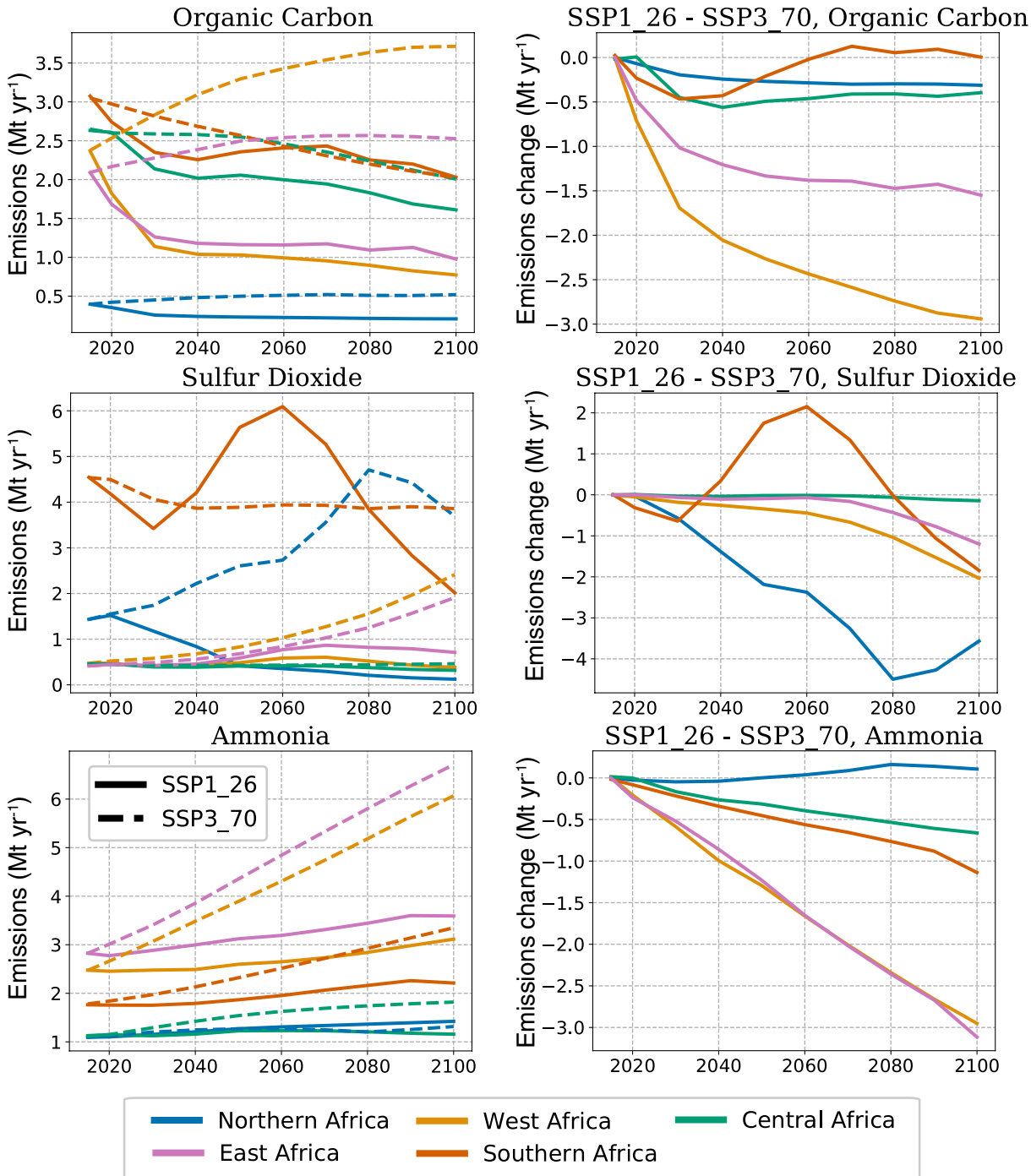

Figure 4. Regional emissions from anthropogenic sources and biomass burning of organic carbon (top row), sulfur dioxide (middle row) and ammonia (bottom row) under the low warming Shared Socio-economic Pathway (SSP1_2.6) and high warming SSP3_7.0 scenarios (left column) and the difference between those (right column). Colors follow the regional map in Figure 2.

4. Current and Future $PM_{2.5}$ Exposure

We examine $PM_{2.5}$ burdens over Africa using 5-year averages to reduce meteorological variability. The spatial pattern of $PM_{2.5}$ loading over Africa reflects both the large emissions sources in some countries such as Nigeria, Egypt, Ethiopia and Uganda/Rwanda/Burundi and the very large amounts of windblown dust in and around the Sahara Desert (Figure 6, left). The differences between the scenarios, however, largely reflect the changes

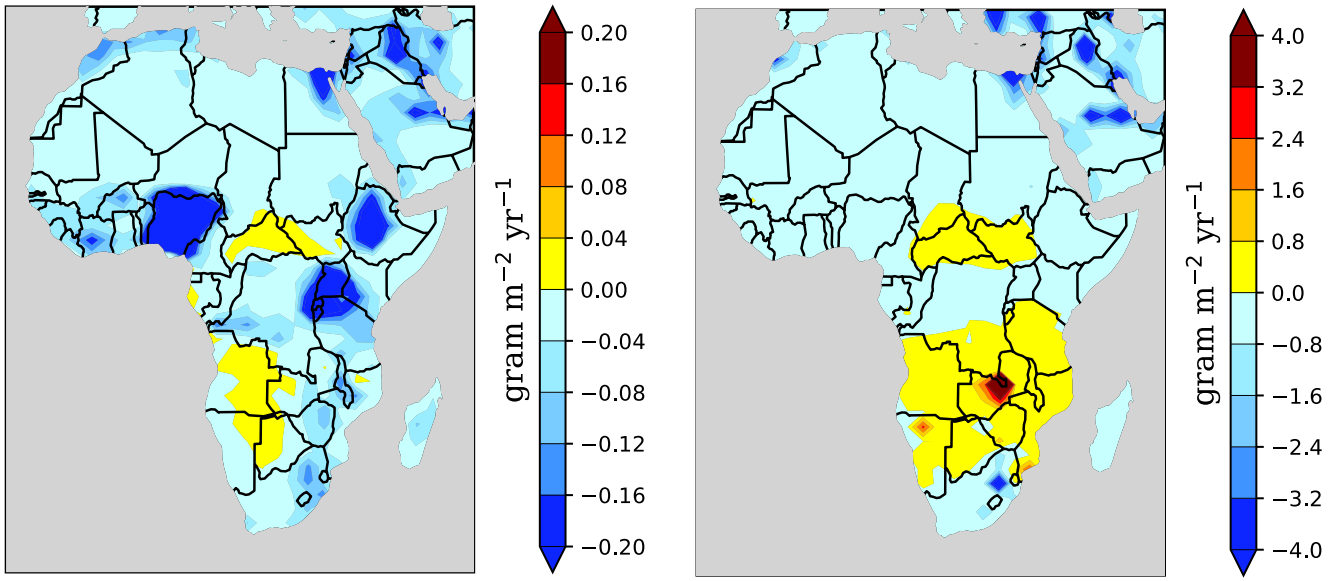

Figure 5. Spatial maps showing the difference of anthropogenic sources and biomass burning emissions of black carbon (left) and sulfur dioxide (right) under the low warming SSP1_2.6 relative to those under the high warming SSP3_7.0 scenario in 2050.

in anthropogenic and biomass burning emissions (Figure 6, right). The models do include changes in dust in response to climate, but these contribute weakly to changes in the multi-model mean. Several individual models show large dust changes (see below), but these are not robust across models and so tend to average out in the multi-model mean.

Turning to the temporal evolution of $PM_{2.5}$ loading, we examine the regional trends in population-weighted exposure (Figure 7). This weighting allows us to concentrate on the $PM_{2.5}$ loading in areas with the highest population density where the health impacts will be largest if there are changes. It is important to note that these

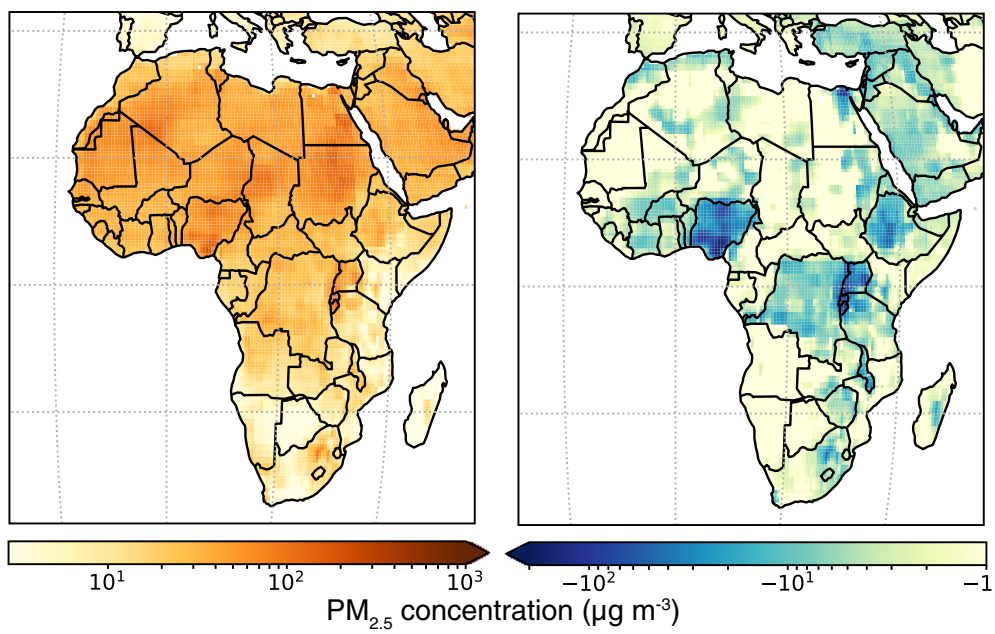

Figure 6. Spatial maps showing the 2015–2019 multi-model (n = 6) mean $PM_{2.5}$ over Africa (left) and the difference between the low warming SSP1_2.6 and high warming SSP3_7.0 scenarios for 2050–2054 (right). Note that the scale is logarithmic.

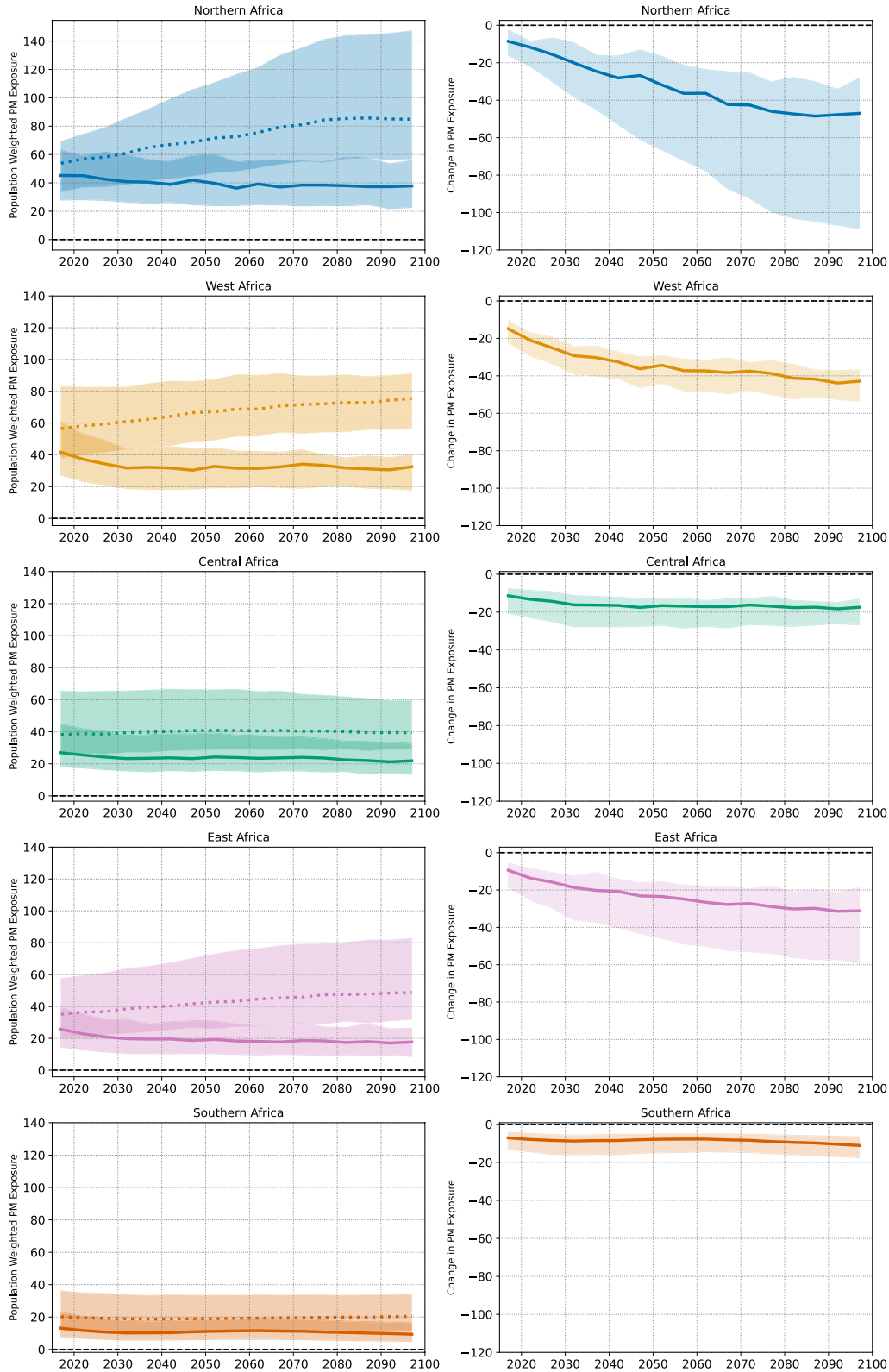

Figure 7. Regional population-weighted $PM_{2.5}$ exposure under the low warming Shared Socio-economic Pathway (SSP1_2.6) and high warming SSP3_7.0 scenarios (left column; μg m^{-3}) and the difference between those (right column; μg m^{-3}) including projected changes in population under those scenarios. The solid lines show the multi-model means and the shaded area shows the full range across the models using the regional colors from Figure 2.

trends include projected changes in population as well as exposure. Changes in population are based on a fusion of country-level future projections for each SSP (Jones & O'Neill, 2016) that are applied to the grid-level 2015 Gridded Population of the World data described in Section 2.

The drop in carbonaceous aerosols appears to play a major role in setting the timing for the $PM_{2.5}$ exposure decreases (Figure 7), likely both because there is a high concentration of those aerosols in Africa and because much of the carbonaceous aerosol burden is exactly where people are located (e.g., due to emissions from biofuel cooking or diesel vehicles). In contrast, ammonia is emitted from agricultural areas, so ammonia concentrations are not coincident with the largest population centers. Additionally, one of the main SO_2 sources is power plants, which again tend not to be geographically as close to people as cookstoves or vehicles. We note that even the first 5-year average (2015–2019) shows decreases in PM2.5 exposure under the low relative to the high warming scenario as the emission scenarios diverge beginning in 2016.

Decreases in $PM_{2.5}$ exposure between the SSP1_2.6 and SSP3_7.0 scenarios are large for East, Northern and West Africa, whereas they are quite modest in Central and Southern Africa. In part this variation in regional benefits reflects the large increases in exposure projected in the first three regions under SSP3_7.0. In East and Northern Africa, the increase in exposure under SSP3_7.0 relative to 2015 is larger than the decrease under SSP1_2.6, indicating that the majority of the benefits in those areas comes from avoiding the rise in pollution exposure under SSP3_7.0. In West Africa the changes relative to 2015 are of similar magnitude under the two scenarios, whereas in Central Africa decreases under SSP1_2.6 are greater in magnitude than increases under SSP3_7.0.

As noted previously, there are large variations in the response of dust aerosols to climate change, leading to a large spread across models in exposure reductions in the low warming versus high warming scenarios in North Africa (Figure 7). This spread is larger than that in any other region in terms of the $PM_{2.5}$ concentration; in relative terms (percent of the multi-model mean reduction) the spreads in Northern, Southern and East Africa are all comparable). This is especially pronounced for the SSP3_7.0 scenario with large amounts of projected warming (~2–3°C relative to 2015 over Africa, in contrast to ~1°C under SSP1_2.6) that are presumably associated with large differences in wind-driven dust emissions in some models.

5. Mortality Impacts of $PM_{2.5}$ Exposure

Following methods used in our prior studies (Shindell et al., 2021), we evaluate the impacts of $PM_{2.5}$ exposure on premature death using the exposure-response functions produced by the Global Exposure Mortality Model which was created from a meta-analysis including 41 cohort studies from around the world, including locations with high-exposures comparable to those in Africa (Burnett et al., 2018). These exposure-response functions yield higher risk increases with increased PM2.5 exposure than earlier analyses, but as they are non-linear it is impossible to give a single value for the increased risk per additional unit exposure. Indicative values are that all-cause risk of premature death increases by about 1% per μg m^{-3} additional exposure for low exposures (<~20 μg m^{-3}), whereas for high exposures (>~60 μg m^{-3}) the increase drops to about half that value. Deaths are evaluated for adults older than 25 using separate risk functions for each 5 years age increment with a low exposure threshold for impacts set at 2.4 μg m^{-3}.

Premature mortalities for a given year attributable to $PM_{2.5}$ exposure are estimated using:

$$\text{Mort} = \text{AF} \times y_0 \times \text{Population} \quad (2)$$

where the attributable fraction AF is defined using the hazard ratio (HR) as (HR-1)/1, y_0 is the all-cause baseline mortality rate and Population is the over 25 years of age local population. The hazard ratio $HR = \exp(\theta T(z))$ incorporates the regression coefficient θ from the meta-analysis and a set of non-linear functions of $PM_{2.5}$ exposure T(z) (Burnett et al., 2018). The uncertainties in this exposure-response function are on the order of ±16% (Burnett et al., 2018). As that uncertainty is systematic across models, we deliberately omit it from our analysis so as to make it clear when the two scenarios' health impacts are statistically different based on the multi-model analysis (see Discussion). Mortalities are evaluated at the grid cell level (0.5 × 0.5°).

Projections of future baseline mortality are from the International Futures (IF, Hughes et al., 2011) model version 7.45 base scenario (http://pardee.du.edu/access-ifs, accessed 23 September 2019). This model projects cause- and country-specific baseline mortality rates through 2100; hence we have a single projection applied across

all scenarios. Those projected baseline mortality rate changes between future years and 2015 are then applied to the grid-level 2015 Global Burden of Disease (GBD) baseline mortality (Stanaway et al., 2018). Population projections in Equation 2 are based on country-level projections for each SSP applied to the grid-level 2015 data as described in Section 4, and do not include changes in age distributions.

The changes in $PM_{2.5}$ exposures as well as changes in population and vulnerability lead to large trends in the $PM_{2.5}$-attributable mortalities in Africa, with large increases under the high warming SSP3_7.0 scenario, stable or decreasing trends under the low warming SSP1_2.6, and therefore large benefits in SSP1_2.6 relative to SSP3_7.0 in all regions (Figure 8). By mid-century, the air pollution co-benefits of climate change mitigation are enormous, with annual premature deaths due to $PM_{2.5}$ reduced by roughly 100,000 in Northern Africa, 175,000 in West Africa, 55,000 in Central Africa, 140,000 in East Africa, and 45,000 in Southern Africa. This totals to ∼515,000 for Africa as a whole in 2050, rising to ∼800,000 near the end of the century. Despite the substantial range in absolute annual deaths across models, the differences between the scenarios are highly statistically significant in all regions (Figure 8). The modeled differences are particularly similar in Northern and West Africa. This may seem counterintuitive given the large range in modeled $PM_{2.5}$ exposures in Northern Africa especially. However, Northern and West Africa experience the highest $PM_{2.5}$ burdens of any region under SSP3_7.0, and as noted previously the impact of each additional microgram decreases as exposure increases so that the much larger $PM_{2.5}$ exposures in some models do not lead to proportionally larger PM-attributable premature deaths. In fact, the ratio of the intermodel spread in premature deaths to the spread in exposure is much lower for those two regions with higher exposure than it is for the other three regions (Table 2). For the same reason, Southern Africa, with the lowest exposures of any region, shows the largest intermodel spread across the multi-model ensemble for health impacts under SSP3_7.0 even though its exposure range is similar to that for Northern or East Africa.

In terms of benefits for public health, reductions in premature deaths are smallest in Central and Southern Africa, in part due to smaller populations but largely because of the weaker decreases in population-weighted $PM_{2.5}$ exposure (Figure 7). These relatively small decreases in exposure outweigh the greater sensitivity at low exposures in those areas. The largest benefits are in West and East Africa, where comparable decreases of 30–40 μg m^{-3} affect the continent's largest populations. The decrease in exposure in Northern Africa is even larger than in West or East Africa, but affects fewer people and occurs through an exposure range over which the response is weaker, leading to smaller absolute impacts than in West or East Africa (though they are still large).

Examining the role of projected changes in population, we find that they have modest impacts in the near-term but are quite substantial in the latter half of the century. For instance, population in most regions is ∼20% larger in 2040 under SSP3 than under SSP1, whereas premature mortalities are typically around 70%–80% greater. Hence the difference in emissions clearly plays a larger role than changes in population in all regions in the first half of the century. By contrast, by the 2090s, population under SSP3 is ∼70%–100% larger than that projected under SSP1, indicating the population change accounts for around ∼66% of the mortality differences during that decade over most regions (with an even higher proportion in Central Africa). In general, emissions changes drive the bulk of the benefits through 2030, with population taking on a gradually larger role thereafter and dominating in the latter half of the century.

Integrating benefits over time, we find that strong climate change mitigation and sustainable development (SSP1_2.6) leads to hundreds of thousands of avoided premature deaths due to $PM_{2.5}$ exposure during the first decade over all regions of Africa (Table 3). The cumulative benefits roughly double by 2040 relative to the values through 2030, with a substantially larger increase during the 2041–2050 period than either of the previous decades. This larger cumulative avoided loss of life in the 2040s reflects both the greater reduction in $PM_{2.5}$ achieved later in the scenarios (Figure 7) as well as the projected changes in population between the two scenarios as discussed previously. Cumulatively by mid-century, the climate change mitigation/sustainable development scenario leads to more than a million avoided premature deaths in every region relative to the baseline scenario, with values exceeding 3 million in East and West Africa. Summing over the entire century, these cumulative values rise to more than 10 million, though as noted the differences in mortalities late in the century are dominated by differences in projected population rather than $PM_{2.5}$ exposure. Given our finding that the "low" group of models agreed better with the ground-based observations and that the model + satellite AOD data appeared to be biased high, we also examined the subset of "low" models (Table 1). The cumulative health benefits are always smaller in this subset than in the full set of models, but by values of 7% or less. Hence the health results are only weakly insensitive to the use of this subset rather than the full ensemble.

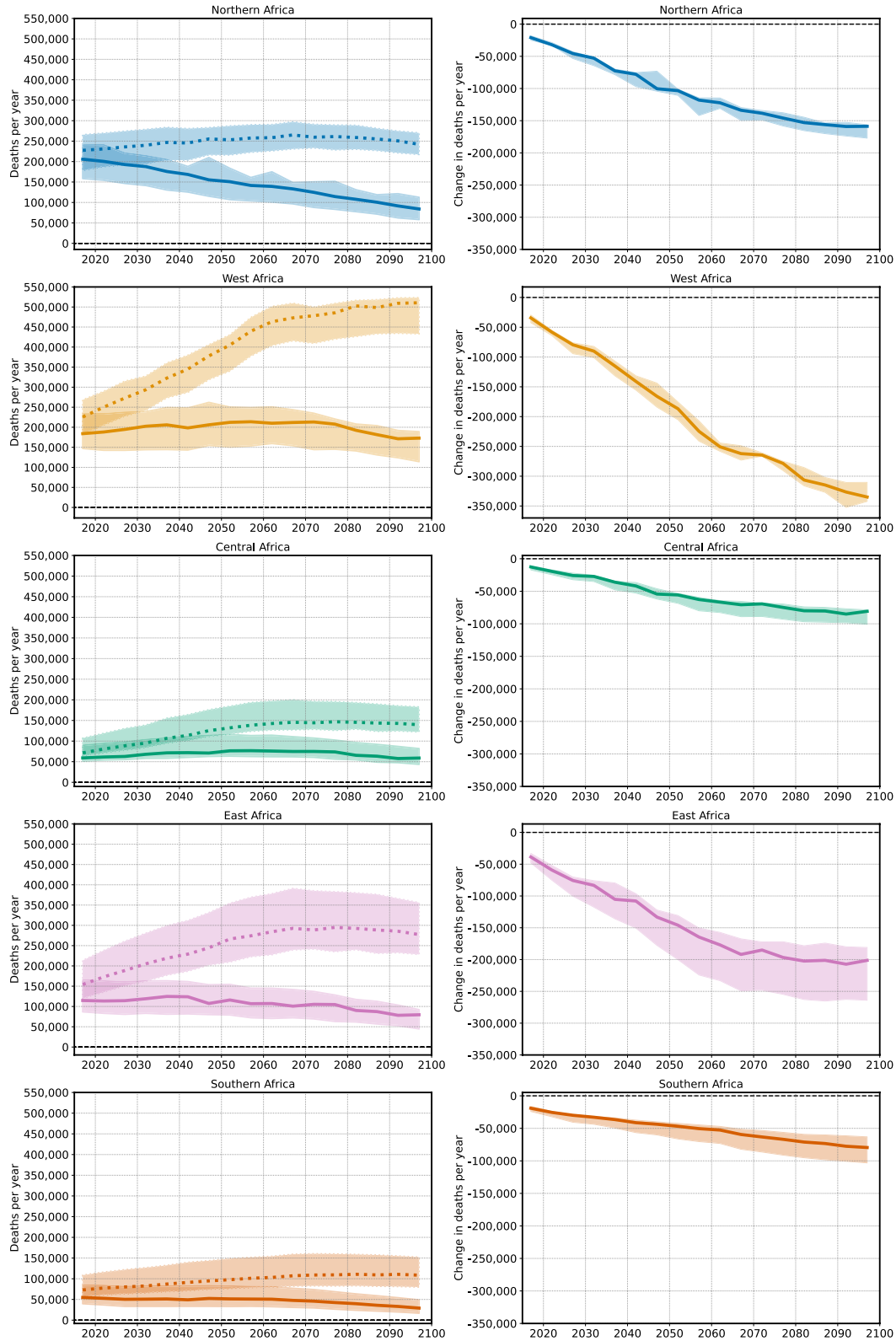

Figure 8. Regional premature deaths due to $PM_{2.5}$ exposure under the low warming Shared Socio-economic Pathway (SSP1_2.6) and high warming SSP3_7.0 scenarios (left column) and the difference between those (right column) including projected changes in population and vulnerability under those scenarios. The solid lines show the multi-model means and the shaded area shows the full range across the models using the regional colors from Figure 2.

Table 2
Population-Weighted $PM_{2.5}$ Exposure and Mortalities Under SSP3_7.0 During 2095–2099

Region	$PM_{2.5}$ exposure mean	Min	Max	Spread	PM mortality mean	Min	Max	Spread	Ratio spread Mortality/exposure
Northern	82.3	58.7	135	46%	248,000	221,000	275,000	11%	0.24
West	74.6	56	90	23%	495,000	437,000	525,000	9%	0.39
Central	37.9	28.1	55.8	37%	144,000	119,000	177,000	20%	0.55
East	47.9	31.4	80.2	51%	284,000	229,000	360,000	23%	0.45
Southern	20.1	11.4	32.8	53%	112,000	80,000	151,000	32%	0.60

Note. Values labeled $PM_{2.5}$ mean and PM mortality mean are multi-model means, whereas Min and Max are the minimum and maximum across the 6 models. The values in columns labeled "Spread" are 100*((max-min)/2)/mean, which give the average of the percent difference between min and mean and max and mean relative to the mean (i.e., the intermodel spread).

6. Discussion and Conclusions

Our analysis examines the $PM_{2.5}$-attributable premature deaths throughout Africa under high and low warming scenarios. We explored the uncertainty in projections of $PM_{2.5}$ exposure through the use of a multi-model ensemble from CMIP6 that serves as a proxy for uncertainties in the Earth system. As noted previously, the roughly ±16% uncertainty in the exposure-response function was omitted so as to make it clear when mortality differences between the scenarios were statistically significant based on the multi-model analysis. However, in all five regions, those uncertainties are less than the multi-model spread (Table 2), and typically much less, indicating that inclusion of those uncertainties would not materially change our results.

We did not incorporate different trends in baseline vulnerability across SSPs. These would, however, likely have a fairly small effect, especially relative to the large differences in population across SSPs. For example, Sellers (2020) shows that the portion of premature deaths in both the Middle East (including North Africa) and Sub-Saharan Africa attributable to chronic respiratory diseases varies quite modestly across the five SSPs in 2040 (the value ranges from ~2.5% to 3.5% of premature deaths for Sub-Saharan Africa and 5%–5.2% for North Africa and Middle East). Future work could include such projections as well as changes in age distributions, though both have substantial uncertainties.

Our analysis explored the consistency of projections of changes in human exposure to $PM_{2.5}$ across a suite of composition-climate models from CMIP6 (Turnock et al., 2020). We found that the full spread of projected regional average exposures across the set of six models ranged from ±20% to ±50% depending on the region (Table 2). In addition, comparison against the limited available observations did not clearly indicate that any of the models performed better than others. This suggests that use of a single model's projections would lead to a highly uncertain result for exposure and that information from a multi-model ensemble is important to provide a good characterization of the range of possible futures for even a well-specified scenario. When examining health impacts, we found the intermodel spread narrowed to about ±10%–30%, depending upon the region, with the intermodel spread in mortality in each region considerably smaller than the intermodel spread in exposure owing to the non-linear exposure-response function that leads to reduced impacts per unit exposure increase at higher exposures (Table 2). Differences in health impacts between the scenarios have even smaller intermodel spreads (5%–25%), especially in Northern and West Africa (Figure 8), as some of the exposure differences between models are systematic across scenarios. Combining these physical uncertainties in mortality estimates with the reported uncertainty in the exposure-response function and treating those as independent leads to a characterization of overall uncertainty in mortalities at a point in time as a range of ±20%–35% whereas for differences between scenarios the range is ±17%–25%.

As noted previously, the future projections studied here include small emissions changes that are already presumed to have taken place over the past ~5 years since those are the scenarios for which projections are available.

Table 3
Cumulative Avoided Premature Deaths Under Shared Socio-Economic Pathway (SSP1_2.6) Relative to SSP3_7.0

Region	2030	2040	2050	2075	2100
Northern	500,000	1,140,000	2,020,000	5,150,000	9,060,000
West	880,000	1,930,000	3,450,000	9,390,000	17,170,000
Central	300,000	630,000	1,120,000	2,820,000	4,900,000
East	890,000	1,870,000	3,140,000	7,630,000	12,810,000
Southern	390,000	750,000	1,200,000	2,640,000	4,550,000

Note. Values are multi-model means.

Alternatively, one could envision the results for any given future year as being likely to occur ~5 years later, though with the worldwide pandemic-related economic slowdown growth in PM-related emissions during 2020–2021 is likely to have been less than that envisioned under the baseline scenario so that values are likely to be only a few years offset. Especially in later years, any offset will have a very small effect on our results.

Our findings regarding the magnitude and range of avoided premature deaths attributable to $PM_{2.5}$ exposure indicate that projected public health benefits can be assessed with relative confidence, especially as benefits are projected to be very large. Actions to mitigate climate change and achieve sustainable development would prevent ~75–100 thousand premature deaths annually in Southern and Central Africa and several hundreds of thousands in the other African regions toward the end of the century. Cumulative benefits through mid-century would exceed 10 million avoided premature deaths for the entire continent, with more than 6 million of those by 2040. Given the value societies place on reduced risk of premature deaths, which is typically in the millions of US dollars per statistical life (Organisation for Economic Cooperation and Development, 2016), these benefits would provide extremely large monetized benefits. The benefits in the near-term are dominated by reduced emissions of air pollutants within Africa, especially those from the energy and residential sectors. These result from transitions away from fossil fuels and traditional biomass fuels in those sectors, respectively, with additional gains from reduced transport and agricultural sector emissions. Longer term benefits stem from both emissions reductions and lower population growth under the low-warming, sustainability scenario.

The size and statistical significance of these effects suggests that policies to address sustainable development and climate change in Africa would benefit from inclusion of public health impacts attributable to air pollution alongside other considerations such as projected changes in drought and heat exposures (Ranasinghe et al., 2021). Public health benefits may be especially salient in Africa, a continent that, given its comparatively small greenhouse gas emissions, has much less control over its future climate than its future air quality.

Conflict of Interest

The authors declare no conflicts of interest relevant to this study.

Data Availability Statement

Resources are available at: the GISS model: https://www.giss.nasa.gov/tools/modelE/; CMIP6 simulations from GISS and other groups: https://esgf-node.llnl.gov/projects/esgf-llnl/; gridded population data: https://sedac.ciesin.columbia.edu/data/collection/gpw-v3; national population projections: https://tntcat.iiasa.ac.at/SspDb/; baseline mortality projections: https://korbel.du.edu/pardee/international-futures-platform/download-ifs.

Acknowledgments
We thank Steven Turnock for CMIP6 surface PM data and the NASA High-End Computing Program through the NASA Center for Climate Simulation at Goddard Space Flight Center and the Duke Compute Cluster for computational resources. We acknowledge the World Climate Research Program for coordinating and promoting CMIP6, the climate modeling groups for producing and making available their model output, the Earth System Grid Federation (ESGF) for archiving the data and providing access, and the multiple funding agencies who support CMIP6 and ESGF. Funding was provided by NASA Cooperative Agreement 80NSSC19M0138.

References

African Union Commission. (2015). Agenda 2063: The Africa we want. In *Addis Ababa, Ethiopia* (ISBN: 978-92-95104-23-5).

Alvarado, M. J., McVey, A. E., Hegarty, J. D., Cross, E. S., Hasenkopf, C. A., Lynch, R., et al. (2019). Evaluating the use of satellite observations to supplement ground-level air quality data in selected cities in low-and middle-income countries. *Atmospheric Environment*, *218*, 117016.

Burnett, R., Chen, H., Szyszkowicz, M., Fann, N., Hubbell, B., Pope, C. A., et al. (2018). Global estimates of mortality associated with long-term exposure to outdoor fine particulate matter. *Proceedings of the National Academy of Sciences of the United States of America*, *115*, 9592–9597.

CIESIN (Center for International Earth Science Information Network). (2005). *Columbia University, united nations food and agriculture programme—FAO, and Centro Internacional de Agricultura tropical – CIATGridded Population of the world, version 3 (GPWv3): Population Count grid*. NASA Socioeconomic Data and Applications Center (SEDAC).

Hughes, B. B., Kuhn, R., Peterson, C. M., Rothman, D. S., Solórzano, J. R., Mathers, C. D., & Dickson, J. R. (2011). Projections of global health outcomes from 2005 to 2060 using the International Futures integrated forecasting model. *Bulletin of the World Health Organization*, *89*, 478–486.

Jones, B., & O'Neill, B. C. (2016). Spatially explicit global population scenarios consistent with the Shared Socioeconomic Pathways. *Environmental Research Letters*, *11*, 084003.

Kelley, M., Schmidt, G. A., Nazarenko, L. S., Bauer, S. E., Ruedy, R., Russell, G. L., et al. (2020). GISS-E2.1: Configurations and climatology. *Journal of Advances in Modeling Earth Systems*, *12*, e2019MS002025.

Mortier, A., Gliß, J., Schulz, M., Aas, W., Andrews, E., Bian, H., et al. (2020). Evaluation of climate model aerosol trends with ground-based observations over the last 2 decades–an AeroCom and CMIP6 analysis. *Atmospheric Chemistry and Physics*, *20*(21), 13355–13378.

Organisation for Economic Cooperation and Development (OECD), & Paris. (2016). *The economic consequences of outdoor air pollution*. 116. https://doi.org/10.1787/9789264257474-en

Petkova, E. P., Jack, D. W., Volavka-Close, N. H., & Kinney, P. L. (2013). Particulate matter pollution in African cities. *Air Quality, Atmosphere & Health*, *6*(3), 603–614.

Ranasinghe, R., Ruane, A. C., Vautard, R., Arnell, N., Coppola, E., Cruz, F. A., et al. (2021). Climate change information for regional impact and for risk assessment. In P. Zhai, A. Pirani, S. L. Connors, C. Péan, S. Berger, N. Caud, Y. Chen, L. Goldfarb, M. I. Gomis, M. Huang, K. Leitzell,

E. Lonnoy, J. B. R. Matthews, T. K. Maycock, T. Waterfield, O. Yelekçi, R. Yu, & B. Zhou (Eds.), *Climate change 2021: The physical science basis. Contribution of working group I to the sixth assessment report of the intergovernmental Panel on climate change [Masson-Delmotte, V.]*. Cambridge University Press.

Riahi, K., Van Vuuren, D. P., Kriegler, E., Edmonds, J., O'Neill, B. C., Fujimori, S., et al. (2017). The Shared Socioeconomic Pathways and their energy, land use, and greenhouse gas emissions implications: An overview. *Global Environmental Change*, *42*, 153–168.

Romanello, M., McGushin, A., Di Napoli, C., Drummond, P., Hughes, N., Jamart, L., et al. (2021). The 2021 report of the Lancet countdown on health and climate change: Code red for a healthy future. *The Lancet*, *398*(10311), 1619–1662.

Sellers, S. (2020). Cause of death variation under the shared socioeconomic pathways. *Climatic Change*, *163*, 559–577.

Shaddick, G., Thomas, M. L., Amini, H., Broday, D., Cohen, A., Frostad, J., et al. (2018). Data integration for the assessment of population exposure to ambient air pollution for global burden of disease assessment. *Environmental Science & Technology*, *52*(16), 9069–9078.

Shindell, D., Faluvegi, G., Seltzer, K., & Shindell, C. (2018). Quantified, localized health benefits of accelerated carbon dioxide emissions reductions. *Nature Climate Change*, *8*(4), 291–295.

Shindell, D., Ru, M., Zhang, Y., Seltzer, K., Faluvegi, G., Nazarenko, L., et al. (2021). Temporal and spatial distribution of health, labor and crop benefits of climate change mitigation in the US. *Proceedings of the National Academy of Sciences*, *118*, 2104061118. https://doi.org/10.1073/pnas.2104061118

Stanaway, J. D., Afshin, A., Gakidou, E., Lim, S. S., Abate, D., Abate, K. H., et al. (2018). Global, regional, and national comparative risk assessment of 84 behavioural, environmental and occupational, and metabolic risks or clusters of risks for 195 countries and territories, 1990–2017: A systematic analysis for the global burden of disease study. *The Lancet, 1923–1994*.

Turnock, S. T., Allen, R. J., Andrews, M., Bauer, S. E., Deushi, M., Emmons, L., et al. (2020). Historical and future changes in air pollutants from CMIP6 models. *Atmospheric Chemistry and Physics*, *20*(23), 14547–14579.

Vohra, K., Vodonos, A., Schwartz, J., Marais, E. A., Sulprizio, M. P., & Mickley, L. J. (2021). Global mortality from outdoor fine particle pollution generated by fossil fuel combustion: Results from GEOS-Chem. *Environmental Research*. https://doi.org/10.1016/j.envres.2021.110754

World Health Organization. (2014). In S., Hales, S., Kovats, S., Lloyd, & D. Campbell-Lendrum (Ed.), *Quantitative risk assessment of the effects of climate change on selected causes of death, 2030s and 2050s*. WHO Press.

World Health Organization. (2016). *Air pollution: A global assessment of exposure and burden of disease*, WHO.